INVESTIGATING THE INFLUENCE OF THE FIELD OF CENTRIFUGAL FORCES ON THE GROWTH AND SEPARATION OF VAPOR BUBBLES IN LIQUID NITROGEN

N. M. Levchenko and I. M. Kolod'ko

UDC 536.248.2.001.5

We have obtained experimental data on the dynamics of bubbles in the injection of vapor through a solitary orifice under conditions of the combined action of an overload ($1 \le \eta \le 260$), of pressure (10^5 Pa $\le P \le 2 \cdot 10^5$ Pa), and of underheating ($0 \le \vartheta \le 4$ K).

The fundamental factors affecting the growth and separation of bubbles in the case of bubbling in a field of centrifugal forces is overload, underheating of the fluid to the saturation temperature, pressure, and the rate of vapor flow. An investigation for the case in which $\eta > 1$ into the formation and separation of gas bubbles in bubbling devices [1] has been undertaken in connection with certain noncryogenic fluids but no generalizing relationships are offered. We know of quantitative relationships governing the growth and separation of bubbles in bubbling without overload [2-5], as well as for boiling in a centrifugal force field (water [6]) and under conditions of terrestrial gravitation in cryogenic underheated fluids [7]. We know of no experimental data on the dynamics of vapor bubble formation in a field of centrifugal forces for cryogenic fluids.

The present study was undertaken with high speed motion-picture photography on an installation similar to that described in [8, 9] (a centrifuge with a vertical axis of rotation). The vaporizer (see Fig. 1), placed into a cryostat with liquid nitrogen, is fabricated out of a glass impregnated plastic material in the form of a cylinder (diameter $12 \cdot 10^{-3}$ m, height $25 \cdot 10^{-3}$ m). A capillary is glued to the upper end and it exhibits an outside diameter of 10^{-3} m and an inside diameter of $6.5 \cdot 10^{-4}$ m. To produce the vapor (by boiling) a heater has been mounted inside, and it is made out of manganin wire. The distance between the capillary to the axis of rotation relative to which the capillary is oriented is r_c = 0.217 m. Such a design provides for stable operation over a wide range of heat flows and angular velocities of rotation.

The experiments were conducted with two heat flows: 0.73 W (overload to η_f = 130) and 3.2 W (η_f = 260). The values of η_f result from the cessation of bubble formation at the orifice to the capillary as a consequence of the increased subcooling, as well as because of a change in the properties of the liquid and the vapor as the pressure rises. Information regarding the experimental conditions can be found in Table 1. Pressure P, subcooling ϑ, and vapor flow rate G (from the motion-picture data) were calculated on the basis of the formulas

$$P = P_A + \int_{r_c - h}^{r_c} \omega^2 r \rho' (P(r),\ T(r))\, dr, \tag{1}$$

$$\vartheta = T_s(P) - T, \tag{2}$$

$$G = V_d / \tau_d \tag{3}$$

with utilization of the thermodynamic properties of the cryogenic fluids [10]. The flowrate values for G_ℓ, calculated on the basis of the thermal balance, exceed the values of the observed flowrate G by 20-30% on the average (see Table 1), which can be explained by the losses of heat and by the condensation of that portion of the vapor discharged into the subcooled liquid. Since an exact estimate of the heat losses is difficult, in the subsequent calculations we will use the given G, and thus the influence of subcooling on the characteristics

Physicotechnical Institute for Low Temperatures, Academy of Sciences of the Ukrainian SSR, Khar'kov. Translated from Inzhenerno-Fizicheskii Zhurnal, Vol. 57, No. 4, pp. 605-610, October, 1989. Original article submitted May 11, 1988.

 0022-0841/89/5704-1196$12.50

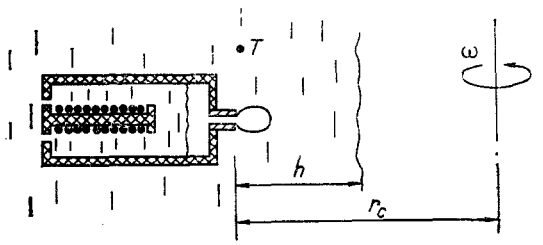

Fig. 1. Diagram of the vaporizer: T) location of temperature sensor, r_c = 0.217 m.

TABLE 1. Experimental Conditions. Characteristics of Bubble Growth and Detachment

η	Q, W	$h \cdot 10^3$, m	$P \cdot 10^{-5}$, Pa	T, K	ϑ, K	$G_l \cdot 10^6$, m^3/sec	$G \cdot 10^6$, m^3/sec
1	0,72	200	1,02	77,4	—	0,78	0,58
6,6	0,75	40	1,03	77,6	—	0,81	0,41
28	0,69	48	1,10	77,9	0,1	0,70	0,43
49	0,72	39	1,14	78,1	0,3	0,71	0,56
103	0,71	53	1,38	78,2	1,8	0,59	0,48
125—130	0,72	40—50	1,41	78,0	2,3	0,56	—
1	3,2	200	1,02	77,4	—	3,57	1,34
22	3,8	53	1,1	78,0	0,1	3,88	3,34
61	3,4	51	1,21	77,9	1,0	3,12	2,50
93	3,6	33	1,25	78,3	1,0	3,28	2,89
137	2,9	37	1,37	78,4	1,5	3,38	2,38
197	2,5	33	1,48	78,2	2,5	1,94	1,44
255—260	3,2	40—50	1,84	79,0	3,8	2,06	—

We	Fr	$R_d \cdot 10^3$, m	f, 1/sec	$\beta \cdot 10^3$, m/sec^n	k
2,65	530	1,15	90	9,6	1,4
0,39	397	0,85	161	8,0	1,4
0,093	10,2	0,64	383	3,1	1,2
0,053	10,1	0,59	645	3,5	1,3
0,025	3,56	0,45	1231	1,5	1,1
0,020	—	—	—	0	—
2,67	2790	1,49	98	19,7	1,8
0,12	791	1,24	413	19,6	1,7
0,043	160	0,98	637	16,2	1,7
0,028	140	0,95	833	7,0	1,5
0,019	65	0,87	855	20,8	1,4
0,013	16	0,65	1235	13,5	1,1
0,009	—	—	—	0	—

being studied will be taken into consideration through the reduction in the vapor flowrate. The resulting injection velocity U is defined as the ratio of the change in bubble volume in the underheated fluid to the lateral cross section of the capillary, i.e., with consideration of condensation in a portion of the vapor flow rate.

The motion-picture photography was carried out at a frame speed of 3000 frames/sec. The bubble dimensions were magnified 5-6-fold. The scale was established on the basis of the capillary image size. Data from 15-20 bubbles were used for each overload value.

The analysis of the photographic materials demonstrated that the increase in the centrifugal acceleration significantly affected the formation and separation of the vapor bubbles. Dimensions were considerably reduced. The bubble shape varied from the pear-shaped with $1 \leq \eta \leq 10$ to the ellipsoidal with a long vertical axis with $10 \leq \eta \leq 50$. In terms of growth time the bubbles were slightly deflected under the action of Coriolis forces in the direction of rotation. The average values for the coefficient of asymmetry can be found in Table 1. During the growth period two-three bubbles merged into large bubbles ($\eta \leq 10$). With further increase in the overload, individual bubbles became detached, and with overloads close to the cessation of bubbling, we observed a certain period of anticipation between a series of bubbles spherical in shape. The increase in the vapor flowrate led to an enlargment of the bubbles and to an increase in the values of η_f. Through this entire mass of experimental data (β, n, τ_d, R_d) we observed significant deviations from the average values, indicating a statistical nature to these quantities.

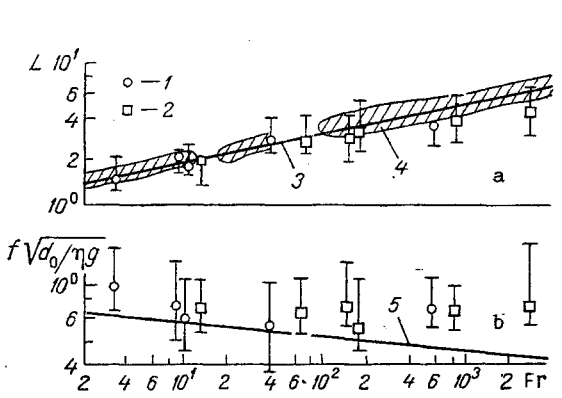

Fig. 2

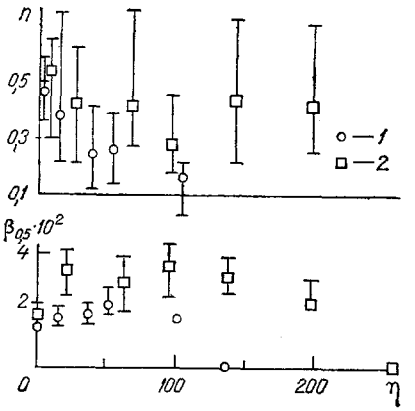

Fig. 3

Fig. 2. Detachment dimension and frequency of bubble detachment as a function of the Fr number: 1) values with Q = 0.69-0.75 W; 2) with Q = 2.5-3.6 W; 3) calculation based on formula (5); 4) experimental data on the dynamic detachment regime in review [2]; 5) calculation based on formula (10); values of the Fr numbers determined with consideration of condensation of a portion of the vapor.

Fig. 3. Exponent n and absolute value of the increase $\beta_{0.5}$ (m/sec$^{0.5}$): the values of 1 and 2 are the same as in Fig. 2; for the conditions of the experiments at the given overloads, see Table 1.

From the equilibrium conditions of the forces acting on the bubble, i.e., buoyancy, hydrodynamic gas pressure, surface tension, and fluid inertia, an equation has been derived in [2] to calculate the detachment size of the bubble as the gas flows into the liquid. We have descriptions of the regimes of bubble formation (statistical, transitional, and dynamic) and approximations of a general equation corresponding to these regimes are given, i.e.,

$$L^5 + \left(\frac{3}{2}\frac{\rho''}{\rho'}\mathrm{Fr} - 6\mathrm{We}\right)L^2 = \frac{\varepsilon_m}{8}\mathrm{Fr}, \tag{4}$$

where $\varepsilon_m = 32$, $\rho' \gg \rho''$.

Let us determine the conditions under which Eq. (4) can be brought to the form

$$L = 1.3\mathrm{Fr}^{0.2}, \tag{5}$$

i.e., the conditions for the existence of the dynamic regime in which the fundamental effect is exerted by the buoyancy force and the force of liquid inertia, and where the effect of the hydrodynamic pressure of the gas is insignificant, consideration of the latter being essential for the case in which $\mathrm{Fr} \gg 4(\rho'/\rho'')\mathrm{We}$ [2].

First of all, the requirement that $L \geq 1$ (the detaching bubble may not be smaller than the supply orifice) imposes a limitation on the minimum value of the Fr number in (5), as a consequence of which

$$\mathrm{Fr} \geqslant 0.27. \tag{6}$$

Secondly, analysis of Eq. (4) shows that the second terms can be neglected if

$$\left|\frac{3}{2}\frac{\rho''}{\rho'}\mathrm{Fr} - 6\mathrm{We}\right| \ll \frac{\varepsilon_m}{8}\mathrm{Fr}, \tag{7}$$

and since $\rho' \gg \rho''$, Fr > 0, We > 0, inequality (7) assumes the form

$$\mathrm{Fr} \gg 1.5\,\mathrm{We}. \tag{8}$$

The conditions of the experiments carried out in the field of centrifugal forces satisfy requirements (6) and (8) (see the Fr, We values in Table 1), and as we can see from Fig. 2, the experimental data are well described by relationship (5) and agree with the known experimental data [2]. With large Fr numbers the experimental values are somewhat lower than the

theoretical, since the growing bubble merges together with the detaching bubbles, never reaching the equilibrium state.

At the instant of detachment, and depending on the overload and the velocity of vapor injection, the bubbles which we had under observation exhibited a variety of shapes. The bubble volume is defined as the volume of an ellipsoid, while the detachment dimension R_d is assumed to be equal to the radius of a sphere of equivalent volume.

The equation for the calculation of the bubble detachment frequency (suggested in [2])

$$f\sqrt{d_0/g} = \frac{3}{2}\mathrm{Fr}^{0,5}L^{-3} \tag{9}$$

for the dynamic regime under overload conditions with consideration of (5) is written as follows:

$$f\sqrt{d_0/\eta g} = 0{,}7\,\mathrm{Fr}^{-0,1}. \tag{10}$$

The experimental data for the frequency of bubble detachment ($f = 1/\tau_d$) are shown in Fig. 2b, with the calculation carried out in accordance with formula (10). We see that relationship (10) is satisfactorily confirmed under conditions of elevated overloads. The merging of the bubbles observed in the case of low overloads (Fr > 500) characterizes the transitional process from the bubble discharge of the vapor to that of a jet, which explains the deviation in the experimental data for f and L from the calculation for the bubble regime.

The relationship between the radius of the bubble growing within the field of centrifugal forces and time, as in the case $\eta = 1$, can be presented in the form

$$R = \beta\tau^n. \tag{11}$$

The modulus of growth β and the exponent n were calculated for each bubble by the method of least squares in the time interval from generation (in the zero frame no bubble yet exists) all the way to detachment, with the reliability of the values based on the Student coefficients in this case amounting to more than 90%.

The average values of β for each overload can be found in Table 1 and the exponent values can be found in Fig. 3. Direct comparison of the growth moduli is impossible because of the variable dimensionality (m/sec^n); the experimental data were therefore processed with the traditional theoretical value n = 0.5 (Fig. 3).

As the overload increased the conditions within the working cavity changed (see Table 1), i.e., we note increases in pressure, subcooling, a reduction in the real vapor flow (in particular, due to the elevated density of the vapor), so that the experimental material in Fig. 3 therefore characterizes the qualitative pattern of the process of vapor formation in the field of centrifugal forces, with the heat flows to the heater remaining constant.

In the case of a large flow the exponent remains virtually constant, i.e., n = 0.4, which is in agreement with the results from our investigation into developed boiling and bubbling [5, 6]. With a smaller flow, the more pronounced effect is exerted by subcooling: the rate of vapor condensation becomes commensurate with the injection velocity and the growth of the bubble prior to separation is retarded (which is borne out with the reduction in n). The reduction in n with increasing subcooling had been noted in the case of boiling in [7].

The absolute value of the growth in comparison with the conditions $\eta = 1$ increases somewhat and with $1 \leq \eta \leq 0.8\eta_f$ remains virtually constant. The reduction in the absolute value of growth ($\eta \gtrsim 0.8\eta_f$) is associated with the reduction in the volumetric flowrate of the vapor. At specific overloads, the formation of bubbles in the capillary ceases (this is designated in Fig. 3b as $\beta_{0.5} = 0$). The rate of bubble growth can be estimated by assuming the velocity of vapor discharge to be constant (determined by the flow rate). The possibility of such a calculation is confirmed by the agreement between the experimental values of the bubble detachment dimensions and the frequencies of bubble detachment with the solutions from [2], based on the relationship $R \sim \tau^{1/3}$.

In conclusion, we should take note of the fact that the theoretical relationships (5) and (10) satisfactorily generalize the experimental results under the condition that the rate of volume increase for the bubbles (the flowrate) makes provision for the condensation of the vapor in the subcooled fluid (in this study this velocity is determined from the motion-picture materials). Additional studies are needed to determine the indirect influence of the subcooling.

NOTATION

a, acceleration at the level of the capillary, m/sec^2; d_0, inside capillary diameter, m; f, frequency of bubble detachment, 1/sec; $Fr = U^2/g\eta d_0$, Froude number; G, vapor flowrate, m^3/sec; g, free-fall acceleration, m/sec^2; h, thickness of the fluid layer above the capillary, m; k, coefficient of bubble asymemtry, equal to the ratio of the larger dimension to that of the smaller at the instant of detachment; $L = 2R_d/d_0$, relative diameter of bubble detachment; P_A, atmospheric pressure, n/m^2; P, pressure at the capillary level, N/m^2; Q, power, W; R, bubble radius, m; r, distance to the axis of rotation, m; r_c, distance from the capillary to the axis of rotation, m; T, fluid temperature at the capillary level, K; T_s, saturation temperature, K; $U = 4G/\pi d_0^2$, vapor discharge velocity, m/sec; V, bubble volume, m^3; $We = \sigma/(\rho' - \rho'')\eta g d_0^2$, Weber number; β, absolute growth value, m/sec^n; $\beta_{0.5}$, absolute growth value for n = 0.5 m/sec$^{0.5}$; $\eta = a/g$, overload; ϑ, subcooling of fluid to saturation temperature, K; ρ', ρ'', densities of the liquid and the vapor, kg/m^3; σ, surface tension, N/m; τ, time, sec. Subscripts: d, on detachment; f, cessation of bubbling.

LITERATURE CITED

1. A. I. Safonov and V. S. Krylov, Teor. Osnov Khim. Tekhnol., 6, No. 1, 51-57 (1972). 2).
2. A. A. Voloshko, A. V. Vurgaft, and V. N. Frolov, Inzh.-Fiz. Zh., 35, No. 6, 1066-1071 (1978).
3. A. A. Voloshko and A. V. Vurgaft, Inzh.-Fiz. Zh., 19, No. 2, 206-210 (1970).
4. A. D. Kondrat'ev, Inzh.-Fiz. Zh., 50, No. 6, 963-969 (1986).
5. N. S. Shcherbakova, Experimental Study of the Growth and Separation of Vapor Bubbles at Artificial Centers of Boiling, Khar'kov (1982). (Preprint: FTINT Akad. Nauk Ukr. SSR; 22-82.)
6. W. A. Beckman and H. Merte, Jr., Trans. ASME, Ser. C, 87, No. 3, 60-68 (1965).
7. Yu. A. Kirichenko and N. M. Levchenko, A Study of the Internal Characteristics of the Boiling of Subcooled Fluids, Khar'kov (1977). (Preprint: FTINT Akad. Nauk Ukr. SSR; 22-77.)
8. N. M. Levchenko, Visualization, Onset of Boiling, and Heat-Transfer Crisises in the Boiling of Cryogenic Fluids. Khar'kov (1986). (Preprint: FTINT Akad. Nauk Ukr. SSR; 12-86.)
9. N. M. Levchenko and I. M. Kolod'ko, Thermal Processes in Cryogenic Systems [in Russian], Kiev (1986), pp. 45-47.
10. V. E. Seregin, A PL-1 Language Program for the Calculation of the Thermophysical Properties of Hydrogen, Oxygen, Nitrogen, and Methane [in Russian], Khar'kov (1985). (Preprint: FTINT Akad. Nauk UKrSSR, 29-95).